Comparative study of two PWM control wind system based on DFIG and multilevel NPC inverter

Etude comparative de deux systèmes éoliens de contrôle MLI basés sur GADA et un onduleur NPC à Multi niveaux

Anis Tarfaya[1,2], Djalel Dib[1,3], Sihem Ghoudelbourk[3] & Mehdi Ouada[1,2]

[1]Department of Electromechanical Engineering, Badji Mokhtar University, PO Box 12, 23000, Annaba, Algeria.
[2]Electromechanical Engineering Laboratory, Badji Mokhtar University, PO Box 12, 23000, Annaba , Algeria.
[3]Department of Electrical Engineering, Larbi Tebessi University, 12000, Tebessa, Algeria.

Article Info

Article history:

Received 13/10/2017
Revised 26/09/2018
Accepted 29/11/2018

Keywords

DFIG, NPC, Multilevel, PWM, THD, Power control.

Mots-clés

GADA, NPC,Multiniveaux, MLI, THD ,Contrôle de puissance.

ABSTRACT

The present paper is a comparative study of two supplying modes of a wind energy conversion system (WECS) based on Doubly Fed Induction Generator (DFIG). This work is conducted with a multi-level neutral-point inverter (NPC) supplying a DFIG.

The first method based on conventional pulse width modulation (PWM) while the second is based on space vector modulation (SVM). This work aimed to control active and reactive power delivered to the electrical networks and satisfying the distribution requirements. The performance evaluation of each method is performed using spectral analysis to calculate total harmonic distortion (THD). Simulation results have showed that the harmonic rate (THD) is reduced. Therefore; the quality of the produced power by this type of wind chain is efficient. The results obtained with SVM have revealed that this technique uses inverter DC bus voltage more efficiently, reduces power losses and minimizes torque ripples.

RESUME

Le présent article propose une comparaison entre deux modes d'alimentation d'un système de conversion d'énergie éolienne (SCEE) basé sur la génératrice à double alimentation (GADA). Il est appliqué à un onduleur multi niveaux à point milieu (NPC). La première méthode est basé sur MLI (modulation de la largeur d'impulsion) conventionnel et le deuxième est basé sur le SVM (modulation de vecteur spatial) .L'objectif visé par ce travail est de contrôler la puissance active et réactive délivré aux réseaux électriques et satisfaire les exigences de cette distribution. L'évaluation des performances de chaque méthode réalisée à l'aide de l''analyse spectrale pour calculer la distorsion harmonique totale (THD).

Les résultats de simulation ont montré que le taux d'harmonique (THD) est réduit. Donc la qualité de puissance produite par ce type de chaîne éolienne est efficace. L'étude de la technique SVM dans les éoliennes révèle que cette technique utilise la tension de bus continue plus efficacement, réduit les pertes de puissance et minimise les ondulations du couple.

Corresponding Author:
Anis Tarfaya
Departement of Electromechanical Engineering,
Badji Mokhtar University, PO Box 12, Annaba, 23000, Algeria.
Email:tarfayaanis@gmail.com

1. INTRODUCTION

Besides to its obvious advantages compared to other conventional types of energy resources, wind energy is one of the most promising and adapted renewable energy for generating electricity in economic terms[1]. Algeria as world major country interests in wind energy and has launched a renewable energy development program. The objective of this program is to achieve 5010 megawatts in 2030 [2]. This demonstrates that wind energy is considered as one of the most challenges research areas in Algeria.

The wind turbines are all based on variable speed operation, using a Doubly Fed Induction Generator (DFIG) or a direct driven synchronous generator (without gearbox) [3].

The DFIG used in several wind energy conversion systems. This machine has proved its efficiency due to qualities such as robustness, cost and simplicity. It offers several advantages, including variable speed operation (±33% around the synchronous speed), and four quadrants active and reactive power capabilities Such system also results in lower converter cost and lower power losses compared to a system based on a fully fed synchronous generator with full-rated converter [4]. Moreover, the generator is robust and requires little maintenance [5, 6, 7, 8, and 9]. For this reason, DFIG become very popular in variable speed wind turbine configurations.

In this system (wind turbine - DFIG), the stator windings are directly connected to the grid, while a frequency inverter interfaces between the standard wound rotor and the grid. In the same way and in wind power systems applied to high voltage, the power supply can be obtained by multi-level voltage inverters (a back-to-back two-level inverters), controlling two variables. The DC-bus voltage and the reactive power accomplished by properly generating the grid current references [10].

In the new universal grid code for wind power generation, the power quality of wind energy is included [11]. For this reason, multilevel inverters controlled by space vector modulation (SVM) are being increasingly preferred for high-power applications [12, 13] such as wind power generation. The multilevel topology not only increases the power rating, but also reduces stress across the switches and improves the voltage waveforms with lower harmonic content.

Despite these advantages of the multilevel inverters, the greatest challenge of this type is the appropriate choice of control type which applies to the power switches. Many research works have been presented with different control schemes of VSI (voltage source inverter applied in a wind energy system [12, 14, 15, 16].

However, these algorithms have the following drawbacks. These techniques are unable to fully utilize the available DC bus supply voltage of the VSI. This technique gives more total harmonic distortion (THD) and does not smooth the progress of future development of vector control implementation of a drive.

Traditionally the sinusoidal PWM technique is widely used in variable speed drive; this algorithm does not smooth the progress of future development of vector control implementation of ac drive. These drawbacks lead to the development of a sophisticated PWM algorithm which is Space Vector Modulation (SVM).This algorithm gives 15 % more voltage output compared to the sinusoidal PWM algorithm [17] thus increasing the DC bus utilization. Furthermore, it minimizes the THD as well as the losses due to the reduction of the inverter commutations number.

This paper presents an ideal combination of the modulation strategy known as SVM technique applied to a three phase three-level VSI in order to optimize the power output. The proposed technique, controls active and reactive powers of the wind turbine based on the DFIG via the control of rotor currents. In the same context and in order to validate this work a comprehensive comparison has been conducted with the conventional PWM technique applied in three phase three-level VSI.

2. MODELING OF SYSTEM COMPONENTS

2.1. General aspect

The three-level NPC inverter was initially presented by Nabae in 1981 [18]. It's illustrated by figure 1. The basic idea of the inverter NPC is to obtain an output voltage at three levels by the superimposing two elementary switches and feeding each by a source of different DC voltage.

The inverter consists of three legs; each leg composed from a pair of semiconductors that are mounted in back to back and two middle diodes to obtain the zero level of inverter output voltage. The midpoint of each arm connected to the midpoint of the DC source.

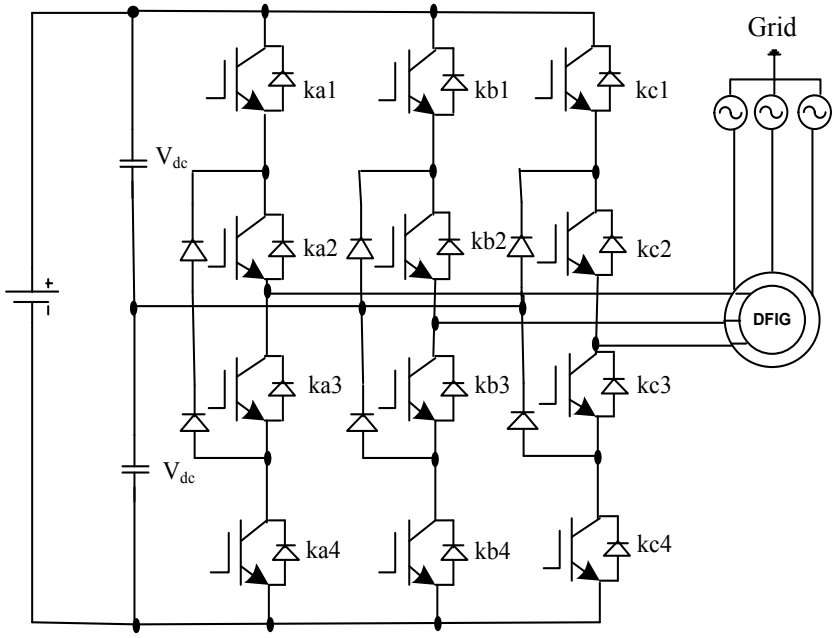

Figure 1: Three level inverter connected to DFIG

To simplify the complexity of the structure of three level-inverter, each pair (Transistor - diode) semiconductors is presented by a single bidirectional switch Sk, and can be seen that, the structure is symmetric. The configuration of a single leg as is shown in figure.2.

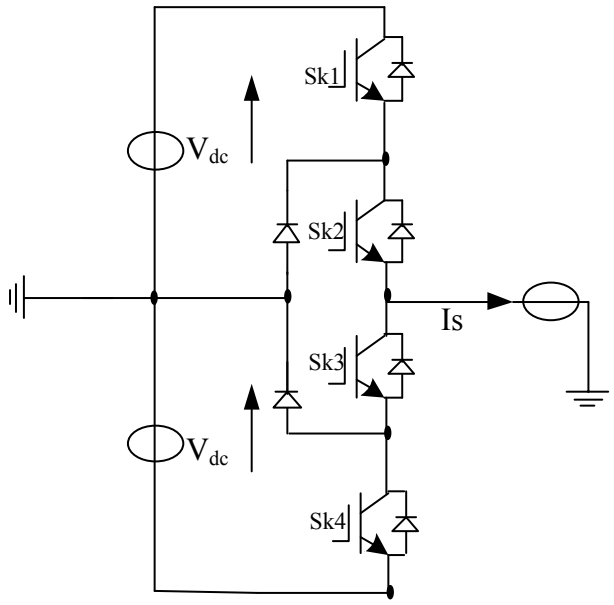

Figure 2 :Three level NPC inverter leg

A leg (k) of the three level inverter can be represented by a switch having three states:
- Sk = -1 for the configuration C0; VKM = -Vdc.
- Sk = 0for the configuration C1, C2, C3; VKM = 0.
- Sk = -1 for the configuration C2; VKM = Vdc.

VKM:This is the voltage at the output of an arm (leg).
The command of switches and the voltages at the output of an arm k of the inverter are given in table 1.

Table 1: Electrical quantities of a k arm of the three-level three-phase inverter

Configuration	K_1	K_2	K_3	K_4	S_k	Voltage at the output of an arm k with regard to the point middle M
C_0	0	0	1	1	-1	$V_{KM} = -U_e$
C_1	0	0	0	0	0	$V_{KM} = 0$
C_2	1	1	0	0	1	$V_{KM} = U_e$
C_3	0	0	1	0	0	$V_{KM} = 0$
C_4	1	0	0	0	0	$V_{KM} = 0$

The voltages at the output of the inverter according to the point (n) are :

$$\begin{pmatrix} V_{an} \\ V_{bn} \\ V_{cn} \end{pmatrix} = \frac{1}{3}\begin{pmatrix} 2 & -1 & -1 \\ -1 & 2 & -1 \\ -1 & -1 & 2 \end{pmatrix}\begin{pmatrix} V_{aM} \\ V_{bM} \\ V_{cM} \end{pmatrix} \quad (1)$$

As: $V_{KM} = S_K U_c$ (2)

Replacing the voltages V_{kM} by their expressions in the equation (1) the phase to neutral voltages applied to the machine become:

$$\begin{pmatrix} V_{an} \\ V_{bn} \\ V_{cn} \end{pmatrix} = \frac{U_c}{3}\begin{pmatrix} 2 & -1 & -1 \\ -1 & 2 & -1 \\ -1 & -1 & 2 \end{pmatrix}\begin{pmatrix} S_a \\ S_b \\ S_c \end{pmatrix} \quad (3)$$

The voltage vector V_s according to sequences S_k and the direct voltage U_c is:

$$V_S = \sqrt{\frac{2}{3}}(V_{an} + aV_{bn} + a^2V_{cn}) = \sqrt{\frac{2}{3}}(S_a + aS_b + a^2S_c)U_c \quad (4)$$

2.2. Modeling of DFIG

In this section we are describing dynamic modeling DFIG in an d,q frame after Parck transformation in order to build numerical simulation in Matlab/ Simulink environment to apply this model was based on simplifying assumption[19].

-Winding is assumed distributed so as to give a sinusoidal EMF if powered by sinusoidal currents.

-The hysteresis, eddy currents and the skin effect is neglected and operation is not in the saturated regime.

- In the end the zero sequence system is zero because the neutral is not connected.

The dynamic model of the DFIG is expressed by the following expressions [20]:

$$\begin{cases} V_{sd} = R_S.i_{Sd} + \dfrac{d\varphi_{sd}}{dt} - \omega_s.\varphi_{sq} \\ V_{sq} = R_S.i_{Sq} + \dfrac{d\varphi_{sq}}{dt} + \omega_s.\varphi_{sd} \end{cases} \quad (5)$$

$$\begin{cases} V_{rd} = R_r.i_{rd} + \dfrac{d\varphi_{rd}}{dt} - (\omega_s - \omega_r).\varphi_{rq} \\ V_{rq} = R_r.i_{rq} + \dfrac{d\varphi_{rq}}{dt} - (\omega_s - \omega_r).\varphi_{rd} \end{cases} \quad (6)$$

Note that "s" and "r" indicate that space vectors are referred to stator and rotor reference frames, respectively. On the other hand, the correlation between the fluxes and the currents in space vector notation is given by the equations (7, 8, and 9).

The DFIG magnetic equations give the flux expressions as follows [21, 22]:

$$\begin{cases} \varphi_{sd} = L_s.i_{sd} + M.i_{rd} \\ \varphi_{sq} = L_s.i_{sq} + M.i_{rq} \end{cases} (7)$$

$$\begin{cases} \varphi_{rd} = L_r.i_{rd} + M.i_{sd} \\ \varphi_{rq} = L_r.i_{rq} + M.i_{sq} \end{cases} (8)$$

The expression of electromagnetic torque based on stator field and currents [23] is given by:

$$C_{em} = P\frac{M}{L_s}\left(\varphi_{sd} i_{rq} - \varphi_{sq} i_{rd}\right) (9)$$

Writing these equations in Park coordinate system that have been used to conduct the vector control making possible the simulation of DFIG in order to facilitate its study and its simulation under MATLAB / SIMULINK.

3. DFIG FED BY THREE-LEVEL NPC INVERTER

The DFIG is studied when is fed by three-level NPC inverter with SPWM and SVM control to show the importance of the control strategy on the inverter performance.

3.1. DFIG fed by three-level NPC inverter with SPWM control

The control signals of the NPC switches were obtained from the intersections of three sinusoidal reference waves shifted by 120 ° and a triangular carrier wave. The algorithm of control is a SPWM (sinusoidal pulse width modulation) for three level inverter is given in Table 2 and Table 3 illustrating the output voltages of three level inverter according to the various configurations of switches.

Table 2: Three level inverter control Algorithm

Test	$U_{refi} \geq 0$		$U_{refi} < 0$	
	$U_{refi} \geq U_{port}$	$U_{refi} < U_{port}$	$U_{refi} \geq U_{por}$	$U_{refi} < U_{port}$
U_{i0}	E/2	0	0	-E/2

The algorithms of control and the results of simulations are obtained when tests were performed for a control index r = Aref/Aport = 0.85 and an index of modulation m = fp/fr = 21.

3.2. DFIG fed by three-level NPC inverters with SVM control

This part deals with the improvement of the control of the indirect power when the DFIG was fed through three level-NPC inverter controlled by SVM with 21 vectors in 13 sectors.

Table 3: Representation of 21vectors

$\frac{de_\alpha}{dt}$	$\frac{de_\beta}{dt}$	S_1	S_2	S_3	S_4	S_5	S_6	S_7	S_8	S_9	S_{10}	S_{11}	S_{12}	S_{13}
0	*0*	v_2	v_3	v_1	*Zvv*	*Zvv*	v_8	v_9	v_{13}	*Zvv*	v_{16}	v_{17}	v_{15}	*Zvv*
1	*0*	v_2	v_3	*Zvv*	v_4	*Zvv*	v_9	v_{10}	*Zvv*	v_{11}	v_{16}	v_{17}	*Zvv*	v_{18}
0	*1*	v_1	*Zvv*	v_6	v_5	*Zvv*	v_8	*Zvv*	v_{13}	v_{12}	v_{15}	*Zvv*	v_{20}	v_{19}
1	*1*	*Zvv*	v_4	v_6	v_5	*Zvv*	*Zvv*	v_{10}	v_{12}	v_{11}	*Zvv*	v_{18}	v_{20}	v_{19}

A combinatorial analysis of all the possible states of the switches has made possible the computation of the components of each voltage vector U_sαet U_sβ. It is then necessary to determine the position of the reference vector in the reference frame α, β and the sector in which it is located. This is limited by the two vectors vi and vi + 1

Table 4: Vector representation of 21 outputs of 3-level inverter in α, β frame

v_{a0}	v_{b0}	v_{c0}	v_α/E	v_β/E	v_{an}	v_{bn}	v_{cn}	v_α/E	v_β/E	$\vec{v}_i$
0	-E/2	-E/2	0.408	0	E/3	-E/6	-E/6	0.408	0	$\vec{v}_1$
0	-E/2	0	0.204	-0.354	E/6	-E/3	E/6	0.204	-0.354	$\vec{v}_6$
0	0	-E/2	0.204	0.354	E/6	E/6	-E/6	0.204	0.354	$\vec{v}_2$
0	0	0	0	0	0	0	0	0	0	$\vec{v}_0$
0	0	E/2	-0.204	-0.354	-E/6	-E/6	E/3	-0.204	-0.354	$\vec{v}_5$
0	E/2	0	-0.204	0.354	-E/6	E/3	-E/6	-0.204	0.354	$\vec{v}_3$
0	E/2	E/2	-0.408	0	-E/6	E/6	E/6	-0.408	0	$\vec{v}_4$
0	E/2	-E/2	0	0.707	0	E/2	-E/2	0	0.707	$\vec{v}_{10}$
0	*-E/2*	*E/2*	*0*	*-0.707*	*0*	*-E/2*	*E/2*	*0*	*-0.707*	$\vec{v}_{11}$
E/2	0	0	0.408	0	-E/6	-E/6	-E/6	0.408	0	$\vec{v}_1$
E/2	0	E/2	0.204	-0.354	-E/6	-E/3	E/6	0.204	-0.354	$\vec{v}_6$
E/2	E/2	0	0.204	0.354	-E/6	E/6	-E/6	0.204	0.354	$\vec{v}_2$
E/2	E/2	E/2	0	0	0	0	0	0	0	$\vec{v}_7$
E/2	- E/2	0	0.612	-0.354	E/2	-E/2	0	0.612	-0.354	$\vec{v}_8$
E/2	0	-E/2	0.612	0.354	E/2	0	-E/2	0.612	0.354	$\vec{v}_9$
E/2	*-E/2*	*-E/2*	*0.816*	*0*	*2E/3*	*-E/3*	*-E/3*	*0.816*	*0*	$\vec{v}_{12}$
E/2	*E/2*	*-E/2*	*0.408*	*0.707*	*E/3*	*E/3*	*-2E/3*	*0.408*	*0.707*	$\vec{v}_{13}$
E/2	*- E/2*	*E/2*	*0.408*	*-0.707*	*E/3*	*-2E/3*	*E/3*	*0.408*	*-0.707*	$\vec{v}_{14}$
-E/2	-E/2	- E/2	0	0	0	0	0	0	0	$\vec{v}_{15}$
-E/2	-E/2	0	-0.204	-0.354	-E/6	-E/6	E/3	-0.204	-0.354	$\vec{v}_5$
-E/2	0	-E/2	-0.204	0.354	-E/6	E/3	-E/6	-0.204	0	$\vec{v}_3$
-E/2	0	0	-0.408	0	-E/3	E/6	E/6	-0.408	0	$\vec{v}_4$
-E/2	*E/2*	*0*	*-0.612*	*0.354*	*-E/2*	*E/2*	*0*	*-0.612*	*0.354*	$\vec{v}_{17}$
-E/2	*0*	*E/2*	*-0.612*	*-0.354*	*-E/2*	*0*	*E/2*	*-0.612*	*-0.354*	$\vec{v}_{18}$
-E/2	*E/2*	*-E/2*	*-0.408*	*0.707*	*-E/3*	*2E/3*	*-E/3*	*-0.408*	*0.707*	$\vec{v}_{17}$
-E/2	*E/2*	*E/2*	*-0.816*	*0*	*-2E/3*	*E/3*	*E/3*	*-0.816*	*0*	$\vec{v}_{16}$
-E/2	*- E/2*	*E/2*	*-0.408*	*-0.707*	*-E/3*	*-E/3*	*2E/3*	*-0.408*	*-0.707*	$\vec{v}_{19}$

The objective of this strategy is to control separately the active and reactive powers produced by the wind turbine and transmitted to the electricity network. This indirect control is based on the space vector by controlling rotor hysteresis currents. The power circuit of this control strategy illustrated in figure 3.

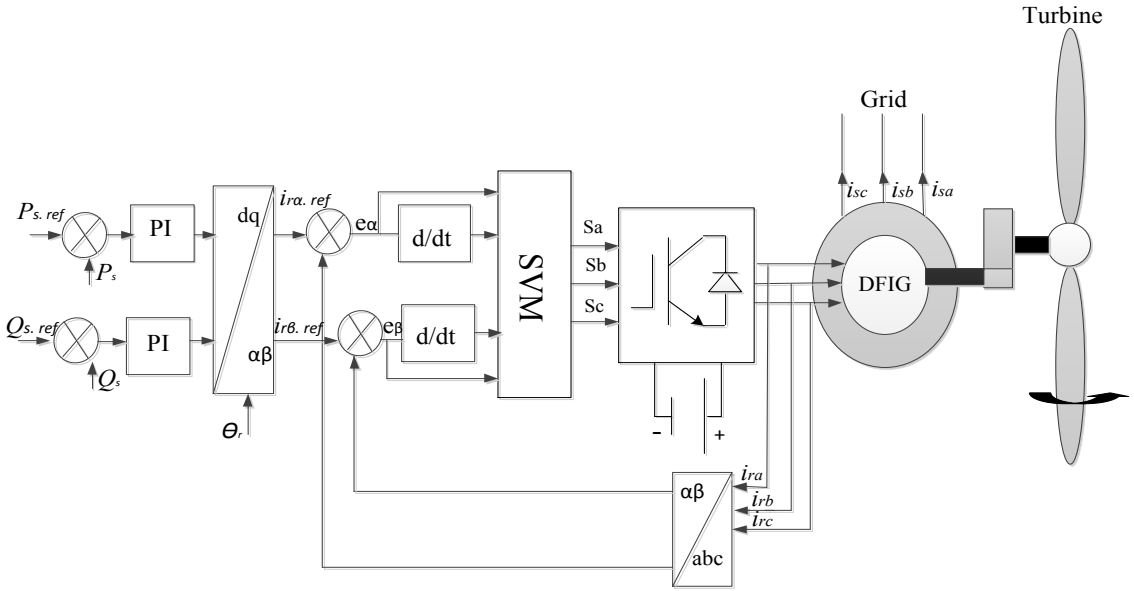

Figure 3: The voltage of DFIG fed by three-level SVM inverter

In this work 13 sectors were defined as shown in figure 4. After several tests, the hysteresis became limited to the following values:

h1/2= 0.445A, h2/2 = 0.47 A , h3 /2= 0.495A.

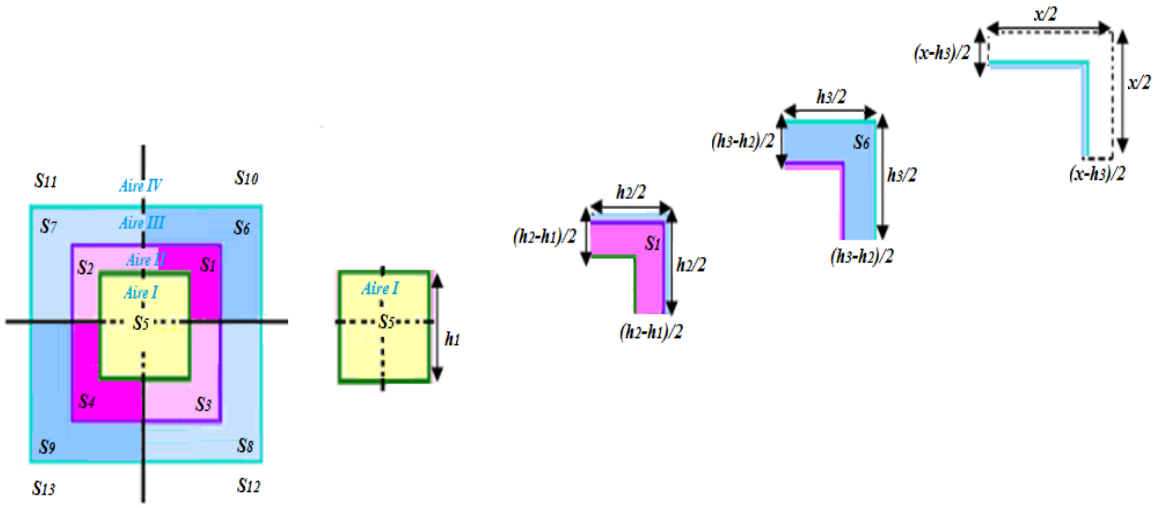

Figure 4 : Representation of 13 sectors

The figure 5 Represents the simulation block under Simulink of GADA fed by three level SVM inverter whilst

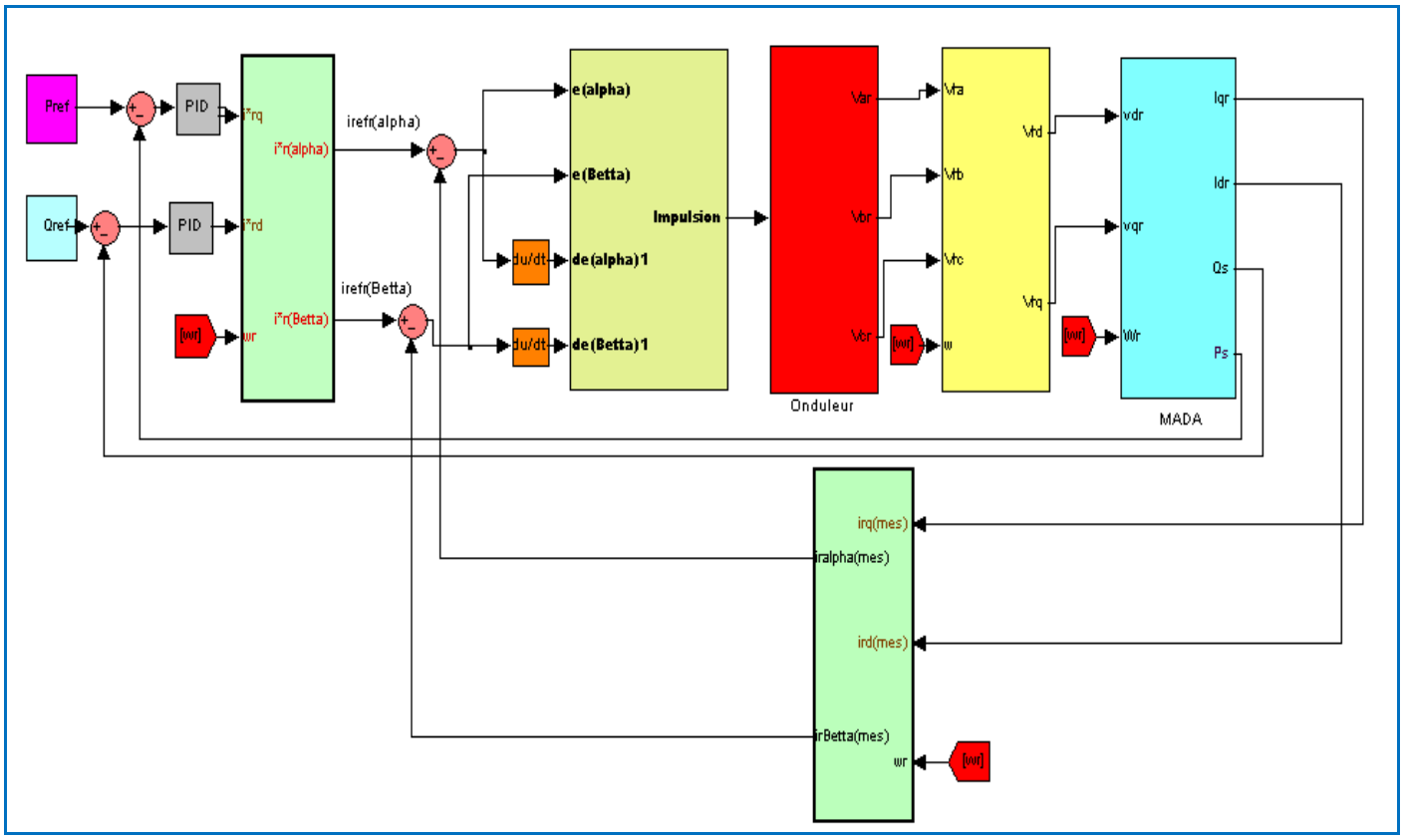

Figure 5 : Simulink block diagram of DFIG fed by three-level SVM inverter

4. RESULTS AND DISCUSSIONS

4.1. The results of WECS simulation based on DFIG controlled by SPWM

The stator of DFIG is directly connected to the grid and the rotor was fed by a three level PWM NPC inverter. The results of simulations were obtained for a constant wind speed (9 m/s) corresponding to a mechanical speed of 120 rad/s. The DFIG supplied by a three level NPC inverter controlled by PWM for a frequency modulation index m=21 and amplitude modulation index r = 0.85. Figure 6.a, illustrates the control signals of multi-level inverter switches.

Figure 6.b, shows the voltage and the rotor current of phase a. It is observed that the shape of the rotor voltage approaches progressively from sinusoidal waveform. Figure 6.c presents the measured active and reactive powers.

These quantities respectively track their reference values and the change of active power at the instants 2s and 4s have no influence on reactive power. The same observation can be made on the change of the reactive power at the instant t = 5s. While, Figure 6.d, presents the torque with fluctuations of ΔC=0.6.Whereas, Figure 6.e presents the evolution of stator current and voltage. According to zooms made on these two values, it is noticed that the frequencies of the voltage and stator current are constant and equal to 50HZ while the amplitudes of the stator voltages are equal to 220v representing conditions of connecting the DFIG to electricity grid. Whereas, the spectral analysis of the stator current with a THD equal to 0.96 % is shown in Figure 6.f.

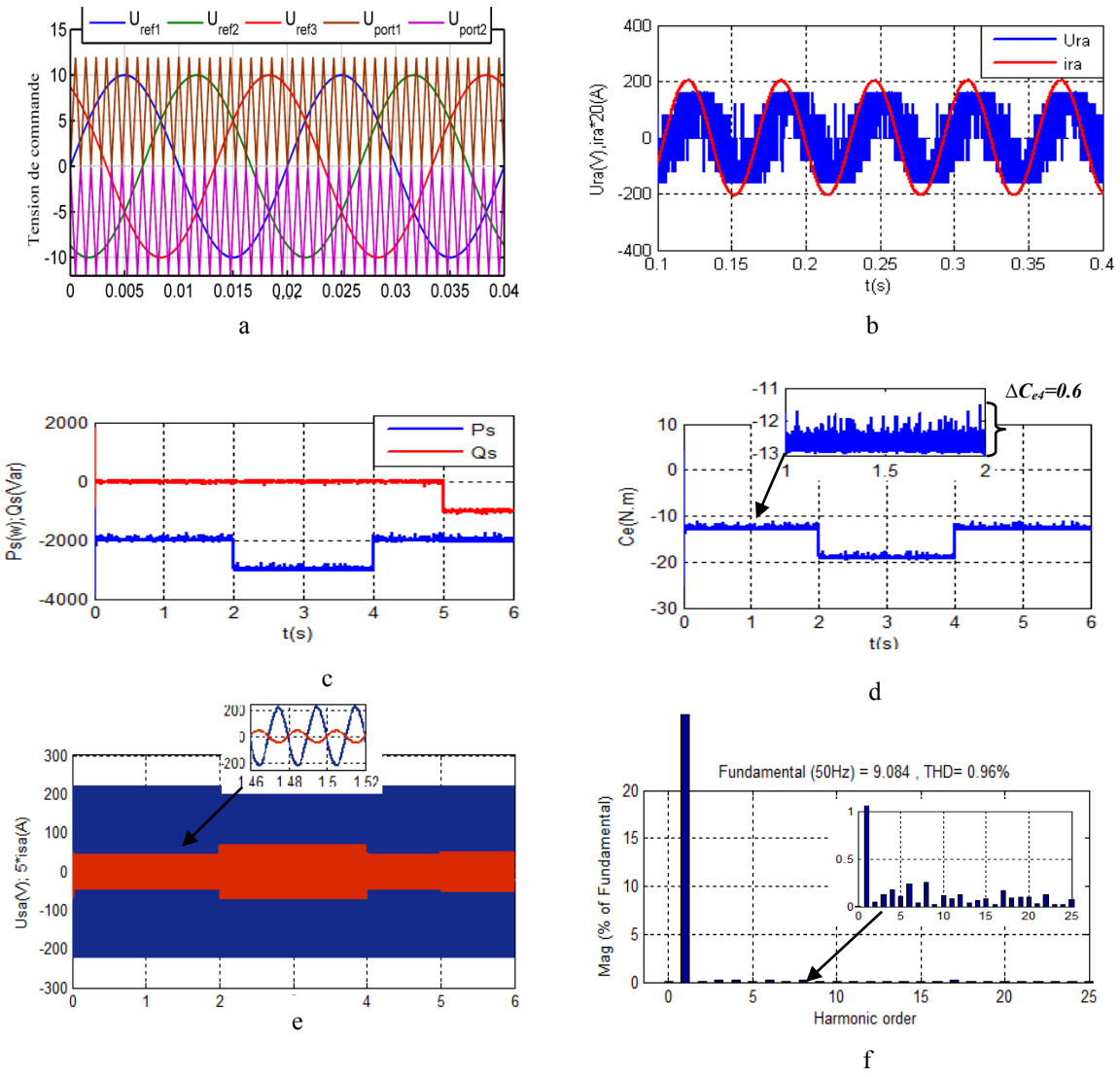

Figure 6 : Simulation results when DFIG is fed by a PWM three-level NPC inverter.
(a) switches control signals, (b) direct voltage Uac, (c) active and reactive power,(d) electromagnetic torque Ce, (e) phase to neutral voltage Usa and stator current isa, (f) Stator current frequency spectrum

4.2. Simulation results of WECS based on DFIG controlled by SVM

Figure 7.a represents areas I; II and III and Figure 7.b the evolution of current will be aligned according to running irβ and we found that it represent a circular path in the plane α, β frame.

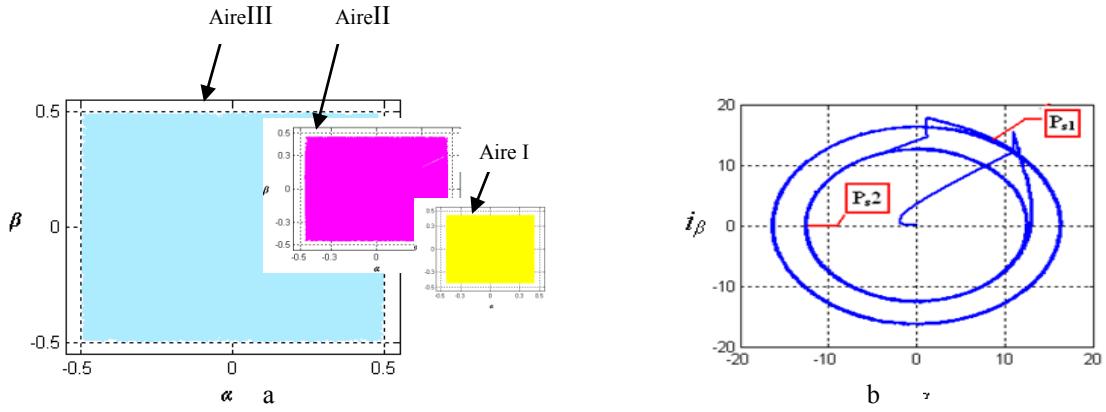

Figure 7: Representation i_α and i_β in α-β frame
(a) Representation of areas, (b) current $i_\alpha$according to i_β

The results of Figure 8.a show that the active and reactive powers are perfectly decoupled, only fluctuations due to modulation control technique, while Figure 8.b presents the torque with an oscillation rate ΔC = 0.3. It is also noted that the three-phase stator current generated by the DFIG are proportional to the supplied active power. The waveform of Figure 8.c the stator current and voltage are almost sinusoidal, which means that good quality of energy supplied to the network is obtained. We notice according to the same figure that the frequencies of stator voltage and current for the period of simulation are constant and equals to 50Hz.While, the amplitude of stator voltage is constant and equal to the network voltage. On the other hand, the amplitude of the current varies with powers variation

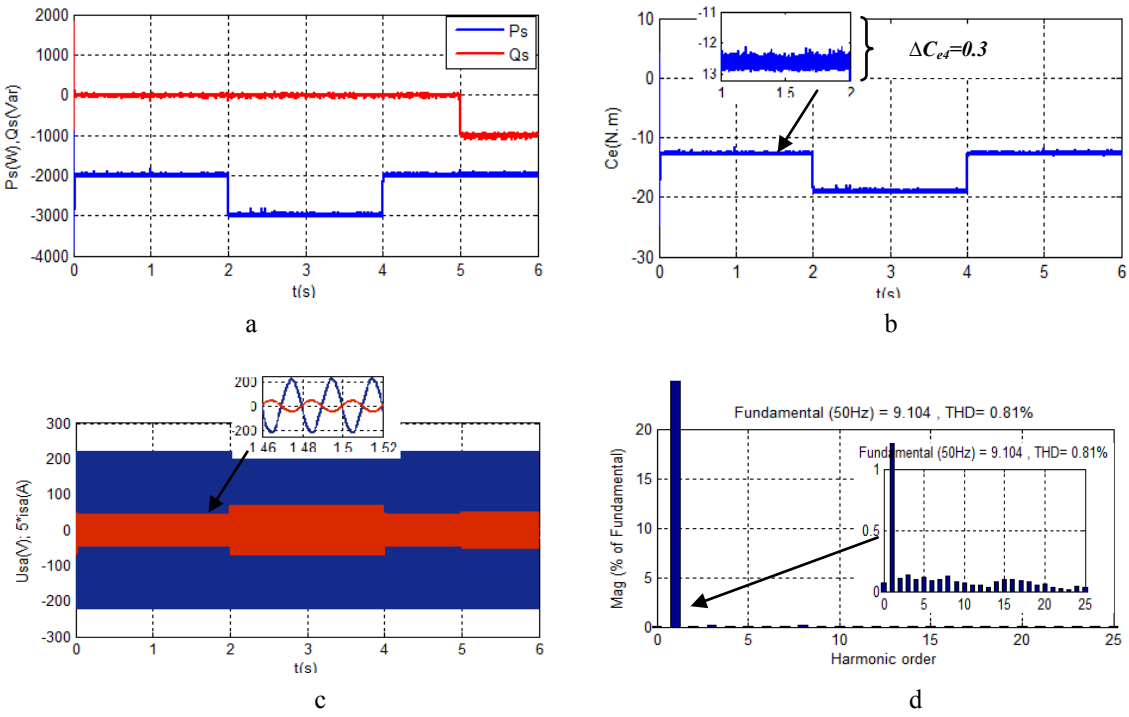

Figure 8 : Results of DFIG fed by three level SVM inverter for sector 21

(a) The active and reactive power, (b) electromagnetic torque, (c) statorique voltage $U_{sa}$and statorique current i_{sa}, (d) Spectral analysis of the stator current

The SVM inverter allows the control of the rotor voltage in amplitude and the phase angle with flexibility. Thus it can be used for the control of DFIG active and reactive power in a wind installation. The control specially designed to reduce harmonic distortion of the stator current generated by the DFIG and the fluctuations of active and reactive powers. reported that the direct control of DFIG active and reactive powers in a wind installation fed by a three level SVM inverter with 21 vectors in 13 sectors. The results obtained with this control strategy gave a stator current with a THD = 0.96 while with the same supply and indirect control of power, it could improve the quality of the stator current (see Figure 8.d THD = 0.81).

5. CONCLUSION

For the control of wind turbine active and reactive powers based on the doubly fed induction generator, the modeling and control of a doubly-fed induction generator based wind turbine-generator system have been considered. More specifically, a new configuration of current control has been presented in this paper. The control scheme was applied on a three-phase and three-level VSI that supplies the rotor winding of DFIG, controlling by that its rotor currents.

The proposed control scheme using SVM was applied to a three-level NPC inverter that supplies the rotor of the DFIG in order to obtain a reduction of harmonic distortion.

For a three-level inverter controlled by SVM strategy using hysteresis controller designed with a control of 21 vectors. The results have showed that a DFIG fed by a three level inverter controlled by SVM has better results compared to DFIG fed a three level inverter controlled by PWM.

The results of comparison have illustrated that the SVPWM modulation has higher amplitude of modulation index and generates less total harmonic distortion (THD) on output voltages. Multi-level

inverters have showed significant advantages over the conventional inverter for medium and high power applications. This is due to their ability to meet the increasing demand of power ratings and power quality associated with reduced harmonic distortion, lower electromagnetic interference, and higher efficiency.

As perspective the present work can be completed by implementing the proposed scheme on reel experimental platform to validate the theoretical developments and simulation results.

ACKNOWLEDGEMENTS

The authors like to thank the Algerian general direction of research DGRDT for their financial support.

REFERENCES

[1] A.M. Eltamaly and H.M. Farh, 2013. Maximum power extraction from wind energy system based on fuzzy logic control.Electric Power Systems Research, Vol. 97, 144-150.

[2] Extrait du portail algérien des energies renouvelables, Objectifs nouveau programme des Energies Renouvelables en Algérie (2015-2020-2030) http://portail.cder.dz/spip.php?article4565 consulted 14/11/2016.

[3] F. Blaabjerg et al., 2012. Power electronics converters for wind turbine systems. IEEE transactions on Industry Applications, Vol.48(2), 708-719.

[4] S. Abdeddaim & A. Betka, 2013. Optimal tracking and robust power control of the DFIG wind turbine. International Journal of Electrical Power & Energy Systems, Vol.49, 234-242.

[5] A.A.B.M. Zin et al., 2013. An overview on doubly fed induction generators′ controls and contributions to wind based electricity generation. Renewable and Sustainable Energy Reviews, Vol. 27, 692-708.

[6] M. Tazil et al., 2010. Three-phase doubly fed induction generators: an overview. IET Electric Power Applications, Vol.4(2), 75-89.

[7] S. Ghoudelbourk et al., 2016. MPPT control in wind energy conversion systems and the application of fractional control (PIα) in pitch wind turbine.International Journal of Modelling, Identification and Control, Vol.26(2), 140-151.

[8] G. Abad et al., 2011. Doubly fed induction machine: modeling and control for wind energy generation (Vol. 85) John Wiley & Sons.

[9] B. Wu et al., 2011. Doubly Fed Induction Generator Based Wecs. Power Conversion and Control of Wind Energy Systems, 237-274.

[10] V. Yaramasu & B. Wu, 2014. Predictive control of a three-level boost converter and an NPC inverter for high-power PMSG-based medium voltage wind energy conversion systems. IEEE Transactions on Power Electronics, Vol.29(10), 5308-5322.

[11] B. Meghni et al., 2017. A second-order sliding mode and fuzzy logic control to optimal energy management in wind turbine with battery storage. Neural Computing and Applications, Vol.28(6), 1417-1434.

[12] H.M. Boulouiha et al., 2015. Direct torque control of multilevel SVPWM inverter in variable speed SCIG-based wind energy conversion system. Renewable Energy, Vol.80, 140-152.

[13] H. Amimeur et al. H., 2012. Sliding mode control of a dual-stator induction generator for wind energy conversion systems. International Journal of Electrical Power and Energy Systems, Vol.42(1), 60-70.

[14] Y. Liu, Y et al., Ge, B., 2011. Quasi-Z-Source inverter based PMSG wind power generation system. In Energy Conversion Congress and Exposition (ECCE), 2011. IEEE, 291-297.

[15] H. Karimi-Davijani et al., 2008. Active and reactive power control of DFIG using SVPWM converter.In Universities Power Engineering Conference, 2008.UPEC 2008.43rd International. IEEE, 1-5.

[16] J. Yao et al., 2008. Coordinated control strategy of back-to-back PWM converter for permanent magnet direct-driven wind turbine J. Automation of Electric Power Systems, Vol.20, 016p.

[17] S. Ananthi et al. 2013. Methods for Varying Speed in Squirrel Cage Induction Motors: A Review. International Journal of Artificial Intelligence and Mechatronics , Vol.1(1), 103-113.

[18] N. Altin and S. Ozdemir, 2013. Three-phase three-level grid interactive inverter with fuzzy logic based maximum power point tracking controller. Energy Conversion and Management, Vol.69, 17-26.

[19] N. Akkari, 2010. contribution à l'amelioration de la robustesse de la commande d'une machine asynchrone a double alimentation, Thèse de Doctorat en Sciences en Electrotechnique, Université de Batna ,Algeria.123p.

[20] Y. Ihedrane et al., 2017. Power Control of DFIG-Generators for Wind Turbines Variable-Speed, International Journal of Power Electronics & Drive Systems (IJPEDS), Vol.8(1), 444-453.

[21] C. Bennour, 2012. Simulation de la commande vectorielle par régulateurs à mode glissant d'une chaîne éolienne à base d'une machine asynchrone à double alimentation, Thèse de Doctorat, Université Mohamed Khider de Biskra, Algeria, 117p.

[22] F. Hachicha & L. Krichen, 2012. Rotor power control in doubly fed induction generator wind turbine under grid faults. Energy, Vol. 44(1), 853-861.

[23] A. Tarfaya et al., 2015. Study Contribution to Control Optimization of a Wind Turbine based on a DFIG. In International Conference on Mechanical and Industrial Engineering (ICMAIE‟ 2015).

NOMENCLATURE

Vsd ,Vsq :	*d-q stator voltage components*
Vrd ,Vrq:	*d-q rotor voltage components*
isd ,isq :	*d-q stator current components*
ird ,irq :	*d-q rotor current components*
φsd ,φsq :	*d-q stator flux components*
φrd ,φrq:	*d-q rotor flux components*
ωs:	*stator angular frequency*
ωr:	*rotor angular frequency*
Cem:	*electromagnetic torque*
Rs:	*stator resistance*
Rr:	*rotor resistance*
Ls:	*stator inductance*
Lr:	*rotor inductance*
M:	*mutual inductance*
P:	*number of pole pairs*
Aref:	*amplitude of the reference voltage (V)*
Aport:	*amplitude of the carrier voltage (V)*
fref:	*frequency of the reference (Hz)*
fport :	*frequency of the carrier(Hz)*
Uio:	*voltage between the phase point i and the middle point (o)*